Improving Photoelectrochemical Performance of PbX (X=S, Se, Te) thin Films by Electro-oxidation for Cu^{2+} Detection

Fuyang Jiang[1,2,], Hongyuan Tang[2], Jishun Li[1,2], Liaoming Yang[2], and Hongcheng Pan[1,2,*]*

[1] Guangxi Collaborative Innovation Center for Water Pollution Control and Water Safety in Karst Area, College of Environmental Science and Engineering, Guilin University of Technology, Guilin, Guangxi, 541006, China;
[2] Guangxi Key Laboratory of Electrochemical and Magnetochemical Functional Materials, College of Chemistry and Bioengineering, Guilin University of Technology, Guilin, Guangxi, 541006, China.
[*]E-mail: panhongcheng@glut.edu.cn, hxd5448_1@163.com

This paper proposes an electro-oxidation method to improve the photoelectrochemical performance of PbX (X=S, Se, Te) thin films electrodeposited onto indium tin oxide (ITO)-coated glass. The PbX/ITO electrode was electro-oxidized using cyclic voltammetry scanning in the potential range of 0-1 V in $NaNO_3$ solution. The photocurrent enhancement was observed in the electro-oxidized PbS/ITO, PbSe/ITO, PbTe/ITO electrodes. Among these three electrodes, the electro-oxidized PbSe/ITO electrode exhibited the strongest, most stable and reproducible photocurrent. The morphology and composition of the electro-oxidized PbSe/ITO electrode were investigated by scanning electron microscopy (SEM) and X-ray powder diffraction (XRD). These results indicate that Se was formed on the surface of the PbSe thin film after the electro-oxidation. The enhancement of photocurrent of the PbSe/ITO electrode could be attributed to the formation of Se-PbSe interface. In a HAc-NaAc buffer solution (pH 5.0), the Se-PbSe/ITO electrode exhibited a good photocurrent response to Cu^{2+} ions, with a dynamic range from 10 nM to 100 μM and the limit of detection of 1.2 nM. The common metal ions at 100 times excess to Cu^{2+} (10 nM) did not interfere with the detection of Cu^{2+} within an error of 10%. The proposed method was applied for the detection of Cu^{2+} in municipal tap, river, and pond water samples, and the results are consistent with those obtained by atomic absorption spectrometry (AAS).

Keywords: Photoelectrochemical performance, Electro-oxidation, PbSe, Se, Cu^{2+} Detection

1. INTRODUCTION

Photoelectrochemical (PEC) sensing is an emerging technology based on the photoelectric conversion characteristics of the semiconductor species. PEC sensing uses direct/indirect interactions between the analyte and the photoelectrochemically active substance, or the photocurrent (or photovoltage) changes generated before and after a biological recognition process for quantitative

detection. The background signal of PEC sensing is lower than that of electrochemical methods. Compared with commonly used spectroscopy methods, the equipment of PEC sensing is simple, inexpensive and easy to miniaturize. Due to these advantages, PEC sensing has attracted more and more attention and has shown promising applications in bioanalysis[1-8], water splitting[9-16], and solar energy conversion[17-19].

Photoelectrochemically active materials are critical to the development of PEC sensors. In the past few decades, although many materials with excellent photoelectrochemical activity (such as TiO_2 and ZnO) have been developed, they are often limited by the low quantum yield because of charge-carrier (e/h) recombination and large band gap.

Lead chalcogenides (PbX, X = S, Se, Te) have been recognized as promising materials for photoelectrochemical sensing due to their narrow direct band gaps (0.32, 0.28, and 0.41 eV of PbTe, PbSe, and PbS, respectively) and high carrier mobilities[4, 20-25]. Wang et al. used PbS quantum dots as photocathodes for photoelectrochemical detection of DNA[26]. Tian et al. developed a photoelectrochemical sensor for lead ion, which is based on the photocurrents of *in-situ* electrodeposition of PbS nanoparticles onto TiO_2 nanotube arrays[27]. Wang et al. used NiO film sensitized with PbS quantum dots as a photocathode to develop an immunosensor for carcinoembryonic antigen[28].

PbX with high photoelectrochemical activity is the key to improve the performance of PEC sensors. Kagan et al. introduced a benzenedithiol and thiocyanate ligands treatment method to enhance the mobility and carriers lifetime in lead chalcogenide thin films, and to improve the photoelectrochemical performance[23]. Jung et al. tailored the PbS/metal interface through the oxide interface layer in Schottky junction to improve the open-circuit voltage and power conversion efficiency[29]. Zhu et al. established an enhanced photoelectrochemical immunosensing platform based on the sensitized structure of TiO_2/CdSeTe@CdS:Mn[30]. TiO_2, CdS, and CdSeTe have cascaded band-edge energy levels, which promotes the ultra-fast transfer of electron-hole pairs and effectively inhibit charge recombination. In addition, because a new band gap is formed by doping Mn^{2+} in CdS, the electron annihilation is significantly suppressed.

Here, we report a simple method to enhance the photoelectrochemical performance of PbX thin films electrodeposited onto indium tin oxide (ITO)-coated glass. In this method, the PbX/ITO electrodes only need to be electrochemically oxidized in an electrolyte solution for hundreds of seconds. After electro-oxidation, the photocurrent of the PbX/ITO electrodes significantly increases. Among the three PbX thin films of PbSe, PbSe and PbTe, the electro-oxidized PbSe films exhibited the strongest, most stable and reproducible photocurrent. In addition, it was found that the photocurrent of the PbSe/ITO electrode decreased with the increase of Cu^{2+} concentration in the solution. On the basis of this founding, we fabricated a highly sensitive and selective PEC sensor for the detection of Cu^{2+} ions in water.

2. EXPERIMENTAL

2.1. Chemicals and materials

$Pb(NO_3)_2$, $NaNO_3$, Na_2SO_4, $Na_2S_2O_3$, SeO_2 and TeO_2 were purchased from Xilong chemical Co. (Shantou, China). NaAc, HAc, and ethylenediaminetetraacetic acid (EDTA) were obtained from

Hongyunlong chemical Co. (Wuhan, China). Ultrapure water (resistivity > 18 MΩ·cm) was obtained from a Milli-Q purification system (Millipore, USA) and was used in all experiments.

2.2. Electrodeposition of PbX onto the ITO electrodes

The PbX thin films were electrodeposited by cyclic voltammetry (CV) with a three-electrode configuration consisting of an ITO electrode as the working electrode, an Ag/AgCl as the reference electrode, and a Pt plate as the counter electrode.

Electrodeposition of PbS: the thin film was electrodeposited by performing cyclic voltammetry from 0.0 to -1.0 V for 80 sweep segments at a scan rate of 0.05 V/s in a solution containing 1mL of 0.2 M $Pb(NO_3)_2$, 1.0 mL of 0.2 M EDTA, 3.5 mL of 0.3 M $Na_2S_2O_3$, and 4 mL of 1.25 M Na_2SO_4.

Electrodeposition of PbSe: the thin film was electrodeposited by performing cyclic voltammetry from 0.0 to -1.0 V for 20 sweep segments at a scan rate of 0.05 V/s in a solution containing 1mL of 0.2 M $Pb(NO_3)_2$, 1.5 mL of 0.2 M EDTA, 3.5 mL of 0.01 M SeO_2, and 4 mL of 1.25 M Na_2SO_4.

Electrodeposition of PbTe: prior to the electrodeposition, the ITO electrode was subjected to a potential of -0.95 V in a 0.1 M H_2SO_4 solution for 30 s, followed by rinsing with water. Then the PbTe thin film was electrodeposited by performing cyclic voltammetry from 0.0 to -1.0 V for 40 sweep segments at a scan rate of 0.05 V/s in a solution containing 1mL of 0.2 M $Pb(NO_3)_2$, 1.0 mL of 0.2 M EDTA, 3.5 mL of 0.01 M TeO_2, and 4 mL of 1.25 M Na_2SO_4.

2.3. Electro-oxidation of the PbX/ITO electrodes

The electro-oxidation of the PbX/ITO electrodes was performed by cyclic potential scanning in the potential range of 0-1 V for 20 segments at a scan rate of 0.1 V/s in a 0.1 M $NaNO_3$ solution.

2.4. Characterization and measurements

Scanning electron microscopy (SEM) analysis was performed on a Hitachi S-4800 scanning electron microscope (Hitachi, Tokyo, Japan). X-ray powder diffraction (XRD) measurements were performed on an X'Pert PRO X-ray diffractometer (Philips, Eindhoven, Netherlands). A CHI 660B (Chen Hua Instruments, Shanghai, China) electrochemical workstation was used for photoelectrochemical measurement with a 300W xenon lamp as the irradiation source. The photocurrent measurement and cyclic voltammetry were performed on a CHI 660B electrochemical workstation (Chenhua, Shanghai, China). All potentials were measured against an Ag/AgCl reference.

3. RESULTS AND DISCUSSION

3.1. Improvement of photoelectrochemical performance of the electro-oxidized PbX/ITO electrodes

The photoelectrochemical performance of the PbX/ITO (X=S, Se, Te) electrodes before and after electro-oxidation were evaluated by measuring the photocurrent under chopped illumination. The

PbS/ITO electrodes exhibited a very weak photocurrent of about 6.5 nA (blue curve in Figure 1a). Under the same experimental conditions, no significant photocurrent was observed for the PbSe/ITO and PbTe/ITO electrodes (blue curves in Figure 1b and 1c).

After electro-oxidation in a 0.1 M $NaNO_3$ solution, the photocurrent of the PbX/ITO electrodes increased (red curve in Figure 1). Both the PbS/ITO and PbSe/ITO electrodes respond to periodic ON/OFF illumination and have a characteristic ''spike and overshoot'' photocurrent transient. An initial sharp photocurrent spike appeared immediately after the illumination was turned on, and then decreased continuously over time until a steady-state value is reached. The photocurrent spikes can be attributed to the separation of electrons and holes at the interface[31-33].
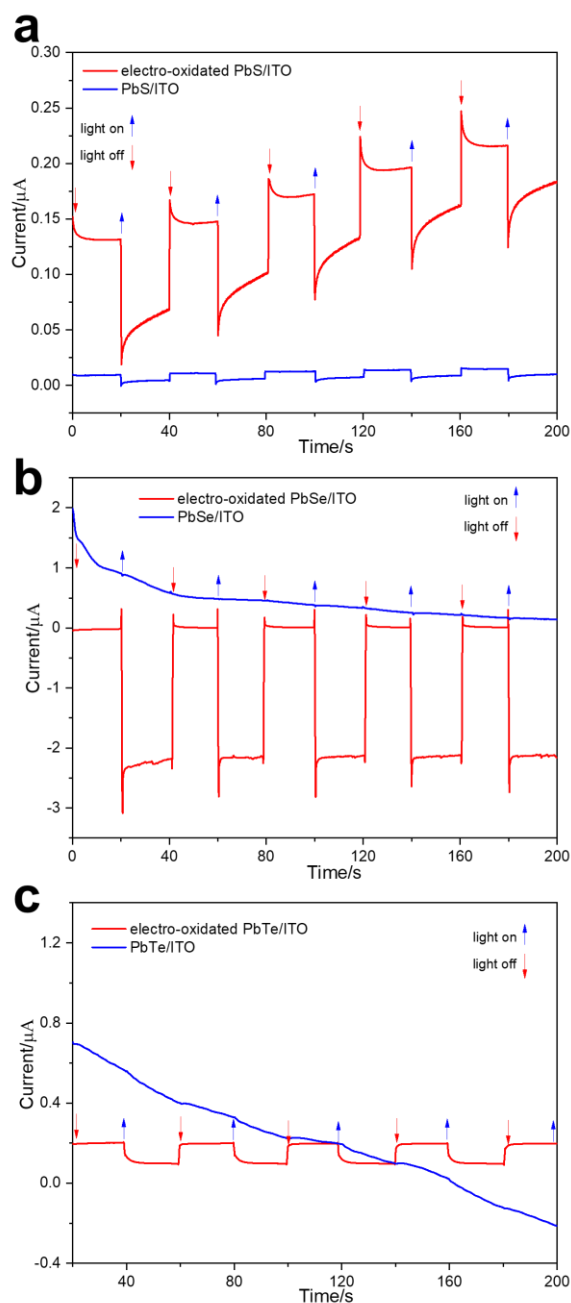

Figure 1. Photocurrent response of the (a) PbS/ITO, (b) PbSe/ITO, and (c) PbTe/ITO electrodes before and after electro-oxidation in a 0.1 M $NaNO_3$ solution. Measurements of photocurrents were performed in a HAc-NaAc buffer solution (pH 5.0) containing 0.1 M $NaNO_3$

The steady-state photocurrent corresponds to the flux of holes, which is successfully transferred to the electrolyte without recombining with electrons on the surface. After the illumination was turned off, an overshoot of the photocurrent is observed. This results from electrons flowing back to the electrode surface to recombine with holes and accumulated holes at surface states[31]. In the case of the electro-oxidized PbTe/ITO electrode, no obvious "spike and overshoot" was observed. The steady-state photocurrent of PbS/ITO, PbSe/ITO and PbTe/ITO electrodes are 0.05, 2.25 and 0.10 μA, respectively. Among the three electrodes, the electro-oxidized PbSe/ITO electrode has the largest steady-state photocurrent and the shortest steady-state time, which is expected to be further applied. Therefore, we take the electro-oxidized PbSe/ITO electrode as a typical example for research.

3.2. Mechanism of the photoelectrochemical performance enhancement

In order to better understand the mechanism of the photoelectrochemical performance enhancement, we used SEM and XRD to study the morphological and compositional changes of the PbSe/ITO electrode before and after electro-oxidation.
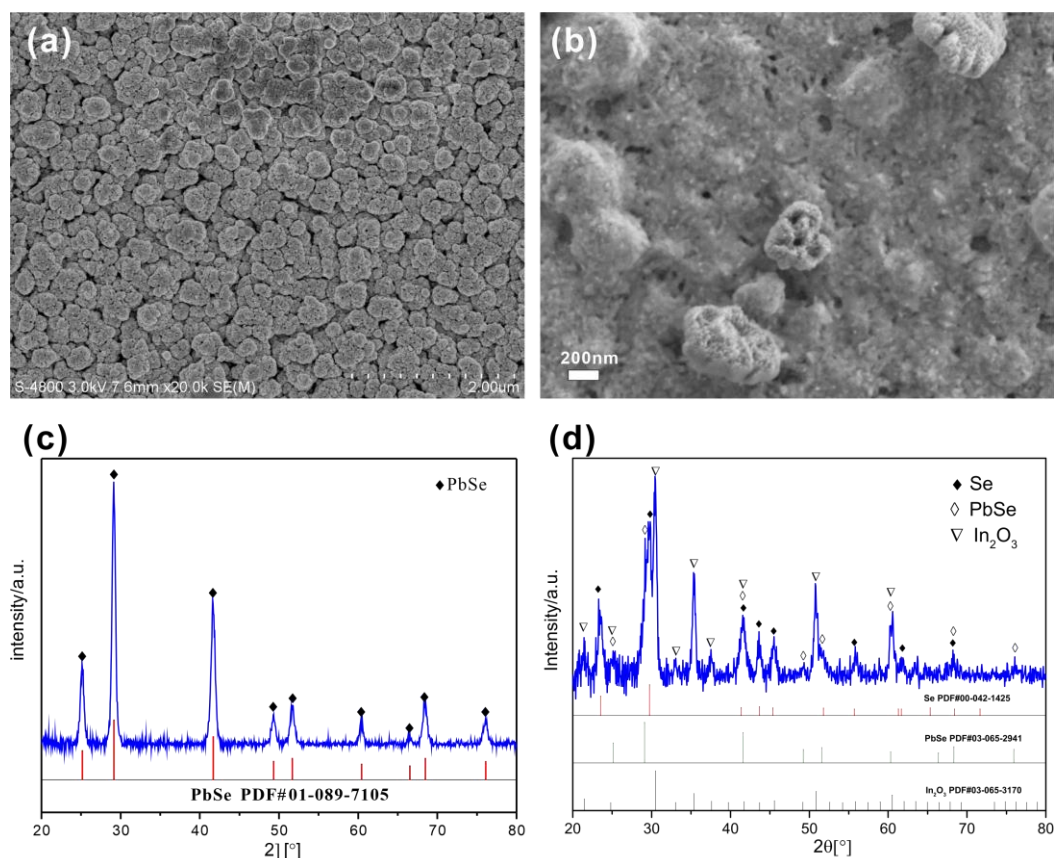

Figure 2. SEM of the PbSe/ITO electrode (a) before and (b) after electro-oxidation; XRD of the PbSe/ITO electrode (c) before and (d) after electro-oxidation by cyclic potential scanning in the potential range of 0-1 V for 20 segments at a scan rate of 0.1 V/s in a 0.1 M $NaNO_3$ solution

Before the electro-oxidation, the SEM image of electrodeposited PbSe shows that the thin film is a granular film with a cauliflower-like structure, composed of spherical particles with a diameter of

hundreds of nanometers, and each particle has numerous nanoscale nodules on its surface (Figure 2a). The XRD analysis in Figure 2c indicates that the strong diffraction peaks at 25.17°, 29.15°, 41.69°, 49.33°, 51.68°, 60.43°, 66.52°, 68.48°, and 76.10° correspond to the (111), (200), (220), (311), (222), (400), (331), (420) and (422) planes of PbSe cubic crystal (PDF#01-089-7105), respectively.

Figure 3 shows the cyclic voltammogram of the electro-oxidation of the PbSe/ITO electrode. During cyclic voltammetric scanning, the PbSe film on the electrode changed from grayish brown to dark brown, indicating that new substances might be formed. As the number of scanning segments increases, the cyclic voltammetric current decreases rapidly, which indicates that the conductivity of the newly generated material on the surface is relatively poor.
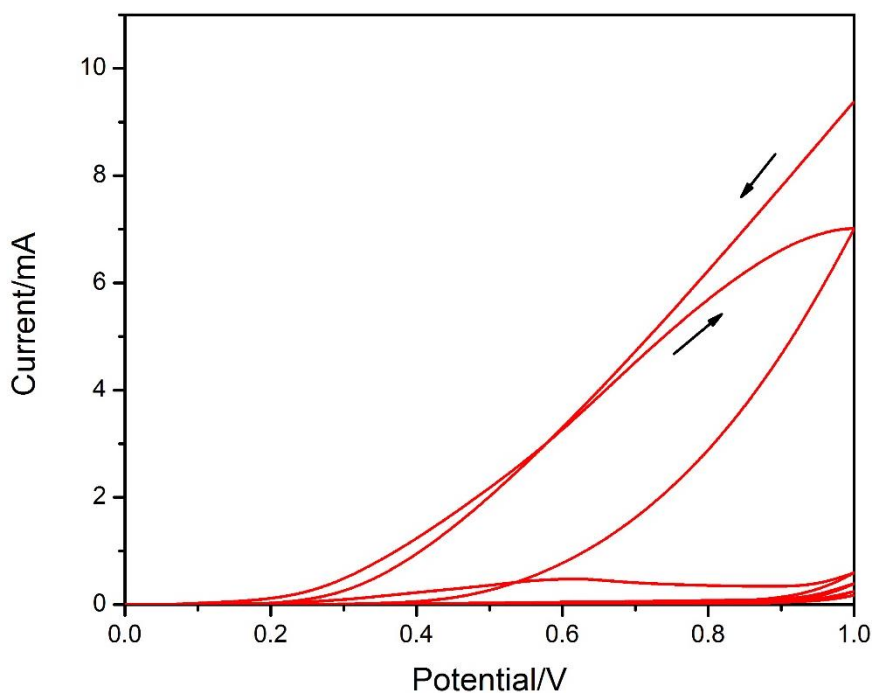

Figure 3. Cyclic voltammogram of the PbSe/ITO electrode by cyclic potential scanning in the potential range of 0-1 V for 20 segments at a scan rate of 0.1 V/s in a 0.1 M $NaNO_3$ solution

After the electro-oxidation, the surface of the granular film was covered with a layer of amorphous material, which reduces the roughness of the film and makes the boundary of the particles unclear (Figure 2b). The XRD patterns of the PbSe/ITO electrode before and after electrooxidation are quite different. As shown in Figure 2d, not only the diffraction pattern of PbSe can be observed, but also the diffraction peaks of the ITO substrate can be observed, which means that the PbSe film becomes thinner or less compact after electro-oxidation. Figure 2d shows that there are some new XRD peaks that cannot be attributed to PbSe and ITO. The new peaks can be indexed to Se (PDF #03-065-2941). Several recently published papers have shown that Se^{2+} in PbSe can be electrochemically oxidized to Se[34-35].

Therefore, the generation of Se can be attributed to the reaction: $PbSe \rightarrow Pb^{2+} + Se + 2e$. These results indicate that the electro-oxidized PbSe thin film is a composite of Se and PbSe.

Previous studies have shown that during annealing in oxygen atmosphere, an oxide layer was formed on the surface of the original PbSe grains. The formation of the oxide layer leads to a significant change in PbSe photoconductivity, which could be well explained by the charge separation[25]. Due to the high conductivity and large carrier lifetime, when Se was coupled with other semiconductors, it can reduce the charge recombination of photo-generated electron-hole pairs[36]. The mechanism of enhanced photoelectrochemical performance might be explained by better charge transfer at the Se-PbSe interface. The interface between Se and PbSe may become a center of charge recombination between holes of Se and photoelectrons of PbSe electrons, thereby promoting the accumulation of photogenerated electrons in Se to the external circuit and generating high photocurrent. This effective charge separation has been observed in a $Se/BiVO_4$ heterojunction[36]. In addition, the surface area of the oxidized electrodes is larger than that of the initial surface, which may be one of the reasons for the increase in photocurrent. Similar photocurrent enhancements were observed on oxidized PbS and PbTe electrodes (Figure 1). It is speculated that the reason may be related to the product and the increase of electrode area after electrooxidation, but further experimental evidence is needed to better understand the possible mechanism.

3.3. Photochemical detection of Cu^{2+} by the Se-PbSe/ITO electrode

We explored the preliminary application of the Se-PbSe/ITO electrode in metal ion sensing. In a certain buffer solution, the Se-PbSe/ITO electrode was used as the working electrode in a three-electrode system, which exhibits a sensitive photoelectrochemical response to Cu^{2+} ion.

We studied the response of the Se-PbSe/ITO electrode to Cu^{2+} ions in different buffer solutions (including citric acid-sodium citrate, Hris-HCl, HAc-NaAc and phosphate buffer). Among these buffer solutions, the Se-PbSe/ITO electrode in the HAc-NaAc buffer solution (pH 5.0) has the most sensitive and stable response to Cu^{2+} ion.

Under the optimal experimental conditions, Figure 4a shows the photocurrent-time curve of the Se-PbSe/ITO electrode at different Cu^{2+} concentrations. We define the value of ΔI as $\Delta I = (I - I_0)/I_0$, where I_0 and I are the photocurrent of the Se-PbSe/ITO electrode in the absence and presence of Cu^{2+} ion, respectively, as the analytical signal. Figure 4b shows that a calibration plot of ΔI versus the logarithm of the Cu^{2+} ion concentration is linear in the range from 10 nM to 100 μM, with a negative slope, the limit of detection of 1.2 nM, and $R^2 = 0.995$.
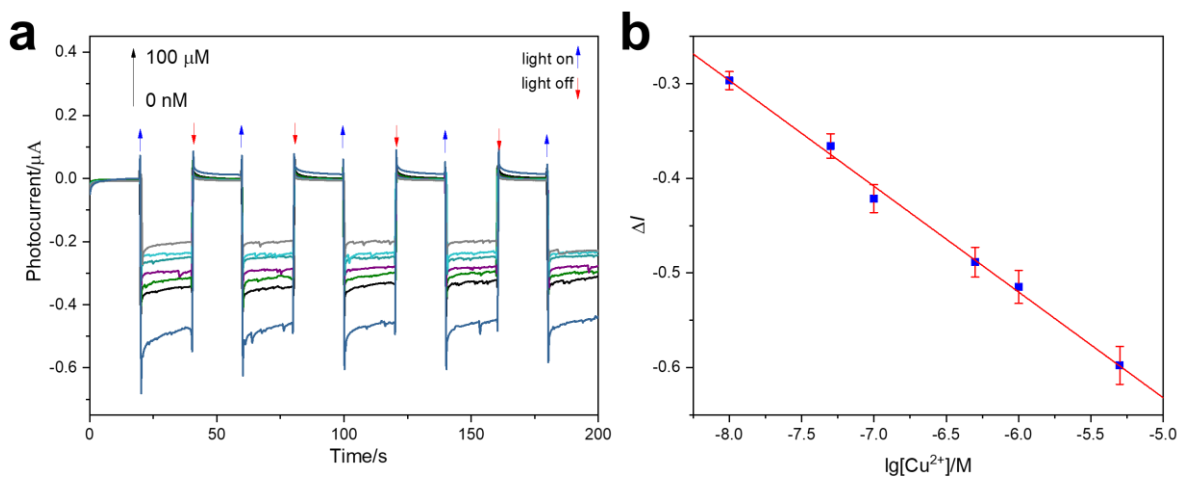
Figure 4. (a) photocurrent-time curve of the Se-PbSe/ITO electrode at different Cu^{2+} concentrations in a HAc-NaAc buffer solution (pH 5.0) containing 0.1 M $NaNO_3$; (b) calibration plot of ΔI versus the logarithm of the Cu^{2+} ion concentration

Several common metal ions, such as Al^{3+}, Fe^{3+}, Mg^{2+}, Ca^{2+}, Mn^{2+}, Zn^{2+}, Cd^{2+}, and Hg^{2+}, were used as potential interferents to evaluate the selectivity of the Se-PbSe/ITO electrode for Cu^{2+} ions. The concentration of interfering ions is 100 water higher than that of Cu^{2+} (10 nM). Figure 6 illuminates the photocurrent response of the Se-PbSe/ITO electrode towards Cu^{2+} and interfering ions. The results show that the relative error of the photocurrent response is less than 10% for all the studied interfering ions whose concentration is 100 times of Cu^{2+}.
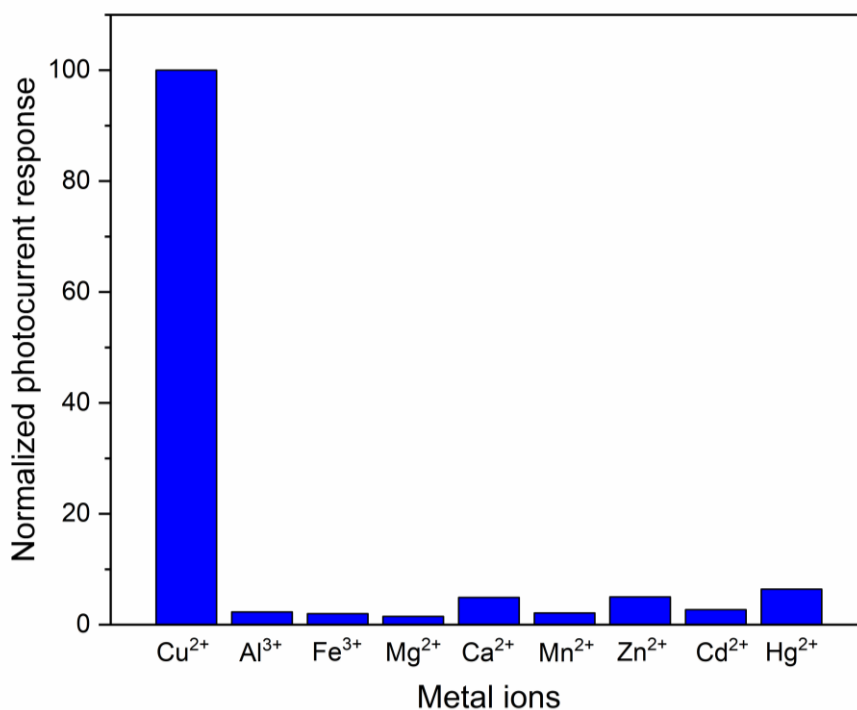

Figure 5. Selectivity for detection of Cu^{2+} (10 nM) in the presence of various interfering ions (1 μM)

The practical applicability of the proposed PEC method was examined to determine Cu^{2+} in real water samples. As shown in Table 1, the concentrations of Cu^{2+} ions in municipal tap water, Li river, and pond water samples measured by the proposed method are in good agreement with the concentration obtained by atomic absorption spectrometry (AAS). The results were also statistically compared by a Student's paired *t*-test. A calculated *t*-test value at a 95% confidence level was found to be 0.609, which is less than the tabulated value of 4.303, indicating that there is no significant difference between the proposed method and AAS.

Table 1. Detection of Cu^{2+} in water samples using the proposed method and AAS

Sample	Cu^{2+}/μg/L	
	Proposed method	AAS
Municipal tap water	3.8	3.2
Li river	4.6	5.2
Pond	5.2	6.0

4. CONCLUSIONS

We found that using cyclic voltammetric scanning in the potential range of 0-1 V, electro-oxidation of PbX thin films electrodeposited onto ITO electrodes in a $NaNO_3$ solution could improve the photochemical performance of the PbX/ITO electrodes. Among the three PbX/ITO electrodes, the PbSe/ITO electrode exhibited the strongest and most stable photocurrent. The SEM and XRD studies of the PbSe/ITO electrodes before and after electrooxidation indicate that the Se-PbSe composite is formed after the PbSe film is electrooxidized. The enhancement in photocurrent of the PbSe/ITO electrode could be attributed to the formation of Se-PbSe interface. The Se-PbSe/ITO electrode exhibited a good photocurrent response to Cu^{2+} ions. On the basis of this, we have developed a PEC method using the Se-PbSe/ITO electrode to detect Cu^{2+} in water. The method has high sensitivity and selectivity, and we demonstrated its effectiveness by detecting Cu^{2+} ions in real water samples. The results are consistent with those obtained by AAS.

References

1. W.-W. Zhao, J.-J. Xu and H.-Y. Chen, *Chem. Soc. Rev.*, 44 (2015) 729.
2. W.-W. Zhao, J.-J. Xu and H.-Y. Chen, *Chem. Rev.*, 114 (2014) 7421.
3. J. Shu and D. Tang, *Chemistry – An Asian Journal*, 12 (2017) 2780.

4. Y.-T. Xu, S.-Y. Yu, Y.-C. Zhu, G.-C. Fan, D.-M. Han, P. Qu and W.-W. Zhao, T*rAC Trends in Analytical Chemistry*, 114 (2019) 81.
5. S.W. Le, Q. Jiang and H.C. Pan, *Int. J. Electrochem. Sci*., 13 (2018) 8960.
6. Y.L. Yuan, G.M. Pang, X.K. Li, W.Y. Zhu and H.C. Pan, *Analytical Methods*, 9 (2017) 5586.
7. H. Tang, J. Zheng, J. Li, Q. Xu and H. Pan, *Optoelectronics and Advanced Materials – Rapid Communications,* 11 (2017) 671.
8. S. Huang, G. Pang, X. Li, J. Li and H. Pan, *J. Nanopart. Res*., 19 (2017) 392.
9. X. Ding, L. Zhang, Y. Wang, A. Liu and Y. Gao, *Coord. Chem. Rev*., 357 (2018) 130.
10. D.K. Lee, D. Lee, M.A. Lumley and K.-S. Choi, *Chem. Soc. Rev., 48* (2019) 2126.
11. S. Wang, G. Liu and L. Wang, *Chem. Rev.,* 119 (2019) 5192.
12. L. Mascaretti, A. Dutta, S. Kment, V.M. Shalaev, A. Boltasseva, R. Zboril and A. Naldoni, *Adv. Mater.,* 31 (2019)1.
13. S. Chandrasekaran, L. Yao, L. Deng, C. Bowen, Y. Zhang, S. Chen, Z. Lin, F. Peng and P. Zhang, *Chem. Soc. Rev*., 48 (2019) 4178.
14. W. Yang, R.R. Prabhakar, J. Tan, S.D. Tilley and J. Moon, *Chem. Soc. Rev*., 48 (2019) 4979.
15. F. Niu, D. Wang, F. Li, Y. Liu, S. Shen and T.J. Meyer, *Adv. Energy Mater*., 10 (2020)1.
16. L. Chen, J. Li, C. Zhou, W. Zhu and H. Pan, *Optoelectronics and Advanced Materials- Rapid Communications*, 8 (2014) 1200.
17. Y. Ping, D. Rocca and G. Galli, *Chem. Soc. Rev.,* 42 (2013) 2437.
18. C. Li, Q. Cao, F. Wang, Y. Xiao, Y. Li, J.-J. Delaunay and H. Zhu, *Chem. Soc. Rev*., 47 (2018) 4981.
19. Z. Yan, M. Ji, J. Xia and H. Zhu, *Adv. Energy Mater*., 10 (2020)1.
20. J. Hu, Y. Shi, Z. Zhang, R. Zhi, S. Yang and B. Zou, *Chin. Physics B*, 28 (2019) 21.
21. E. Esakkiraj, K. Mohanraj, G. Sivakumar and J. Henry, *Optik*, 126 (2015) 2133.
22. Y. Dong, S. Xia, P. Jiang, G. Wang and S. Zhao, *New J. Chem.,* 42 (2018) 2243.
23. S.J. Oh, D.B. Straus, T. Zhao, J.H. Choi, S.W. Lee, E.A. Gaulding, C.B. Murray and C.R. Kagan, *Chem. Commun*., 53 (2017) 728.
24. L.-N. Qiao, H.C. Wang, Y. Shen, Y.-H. Lin and C.-W. Nan, *Aip Advances*, 6 (2016) 37.
25. Y.X. Ren, T.J. Dai, W.B. Luo and X.Z. Liu, *Vacuum*, 149 (2018) 190.
26. G.-L. Wang, K.-L. Liu, J.-X. Shu, T.-T. Gu, X.-M. Wu, Y.-M. Dong and Z.-J. Li, *Biosens. Bioelectron.,* 69 (2015) 106.
27. Y. Luo, C. Dong, X. Li and Y. Tian, *J. Electroanal. Chem*., 759 (2015) 51.
28. Y.-T. Gong, X. Wu, Y. Dong, Q. Liu, Z. Li and G.-L. Wang, *Sens. Actuators*, B., 266 (2018) 408.
29. M.-J. Choi, J. Oh, J.-K. Yoo, J. Choi, D.M. Sim and Y.S. Jung, *Energy Environ. Sci*., 7 (2014) 3052.
30. G.-C. Fan, H. Zhu, D. Du, J.-R. Zhang, J.-J. Zhu and Y. Lin, *Anal. Chem*., 88 (2016) 3392.
31. M. Rohloff, B. Anke, S. Zhang, U. Gernert, C. Scheu, M. Lerch and A. Fischer, *Sustainable Energy & Fuels,* 1 (2017) 1830.
32. M. Mokhtarimehr and S.A. Tatarkova, *J. Opt. Soc. Am. B: Opt. Phys*., 34 (2017) 1705.
33. L.M. Peter, *J. Solid State Electrochem*., 17 (2012) 315.
34. W. A. Rodriguez-Rodriguez, J. Colon, R. Guzman, H.Rivera, M. E. B. Santiago-Berrios, *Mater. Res. Express*, 1 (2014) 035906.
35. X. Chen, Y.-B. Zhu,; Z. Xing, G. Tang, H. Fan, *J. Mater. Sci.: Mater. Electron.*, 27 (2016) 1151.
36. S.N.F.M. Nasir, H. Ullah, M. Ebadi, A.A. Tahir, J.S. Sagu and M.A.M. Teridi, *J. Phys. Chem*. C, 121 (2017) 6218.